creative commons
COMMONS DEED

저작자표시-비영리-변경금지 2.0 대한민국

이용자는 아래의 조건을 따르는 경우에 한하여 자유롭게

- 이 저작물을 복제, 배포, 전송, 전시, 공연 및 방송할 수 있습니다.

다음과 같은 조건을 따라야 합니다:

저작자표시. 귀하는 원저작자를 표시하여야 합니다.

비영리. 귀하는 이 저작물을 영리 목적으로 이용할 수 없습니다.

변경금지. 귀하는 이 저작물을 개작, 변형 또는 가공할 수 없습니다.

- 귀하는, 이 저작물의 재이용이나 배포의 경우, 이 저작물에 적용된 이용허락조건을 명확하게 나타내어야 합니다.
- 저작권자로부터 별도의 허가를 받으면 이러한 조건들은 적용되지 않습니다.

저작권법에 따른 이용자의 권리는 위의 내용에 의하여 영향을 받지 않습니다.

이것은 이용허락규약(Legal Code)을 이해하기 쉽게 요약한 것입니다.

Disclaimer

dCollection

전 용 필 교수지도

석사학위 청구논문

The effects of the interaction of alternatively spliced β-catenin with prion protein in embryo development during early pregnancy

2025

성신여자대학교 대학원

생물학과

장 예 림

The effects of the interaction of alternatively spliced β-catenin with prion protein in embryo development during early pregnancy

A Master's Thesis

Submitted to the

Graduate School of Sungshin University

In partial fulfillment of the requirements

for the degree of master of biology

Ye rim Jang

Feb, 2025

This is certify that we have examined the

Master's Thesis of

Ye rim Jang

Submitted to Department of Biology

Approved as to style and content:

Thesis Advisor ..... Yong pil Cheon

Committee Chairman ..... Byoung Joon Ko

Committee Member ..... Sung Ho Lee

Committee Member ..... Yong pil Cheon

The Graduate School of Sungshin University

ABSTRACT

The effects of the interaction of alternatively spliced β-catenin with prion protein in embryo development during early pregnancy

Ye rim Jang

Department of Biology

Graduate School of

Sungshin University

Embryo implantation is a process of interaction between the differentiating uterine stromal cells and gastrulating embryo. Even though β-catenin is known as an factor for implantation its molecular works are not much unmasked. In this study, we explored the interaction of β-catenin, a key effector of the Wnt signaling pathway of decidualization with cellular prion protein (PrP^c), a multifunctional protein, during pregnancy. While β-catenin

maintained stable expression in epithelial regions from Days 1 to 5, PrP^c exhibited lower but showed parallel expression patterns. On Days 6 and 7, β-catenin expression decreased toward deeper uterine zones, whereas PrP^c showed increasing expression in deep zones. β-catenin and PrP^c exhibited distinct spatiotemporal expression patterns during early pregnancy. β-catenin showed stable expression in luminal and glandular epithelium from Days 1–5, decreasing across decidual zones on Days 6–7. PrP^c increased toward deeper decidual zones. Both proteins were prominent in stromal cells, with β-catenin favoring undifferentiated stromal cells and PrP^c strongly expressed in decidualized cells. These findings suggest β-catenin and PrP^c act as transcriptional co-activators critical for stromal cell differentiation during decidualization. Co-immunoprecipitation experiments revealed that PrP^c co-precipitates with β-catenin, confirming their interaction. This suggests that the β-catenin–PrP^c complex may play a crucial role in uterine development and implantation during early pregnancy. Single cell RNA sequencing identified two major β-catenin isoforms: the canonical form and the intron retention form. The canonical form exhibited decidualization-dependent expression, while the intron retention form was estrogen-dependent. Using the $Prnp^{ZH3/ZH3}$ knockout mouse model, we confirmed that PrP^c interacts

specifically with the canonical β-catenin isoform. PrP^c-null mice exhibited impaired decidualization and altered β-catenin isoform expression, highlighting the importance of this interaction.

These results reveal a critical interplay between β-catenin and PrP^c during implantation, and suggests distinct roles for β-catenin isoforms in uterine stromal differentiation and embryo development.

CONTENTS

List of Tables

List of Figure

INTRODUCTION

The β-catenin protein (CTNNB1) (Figure 1), a crucial molecule of the canonical Wnt pathway, plays an important role in cell adhesion, development, transcription, and tumorigenesis. In the absence of the Wnt signal, β-catenin is captured by the GSK3β (glycogen synthase kinase 3β) destruction complex which bound to axin (a bridging molecule). And when the S33 and S37 sites of β-catenin are phosphorylated by GSK3β, it is rapidly ubiquitinated from the N-terminus by an E3 ligase containing an F-box protein called β-transducing repeat containing (BTRC) protein, and degraded by the proteosome. (Kitagawa et al., 1999) On the contrary, in the presence of the Wnt signal, the function of the destruction complex is inhibited, and β-catenin is not phosphorylated. Free β-catenin undergoes cytoplasmic accumulation and translocation to the nucleus, where it binds to transcription factors called TCF/Lef, activates the transcription of Wnt target genes, and promotes physiological processes such as cellular proliferation and apoptosis. Therefore, β-catenin with dephosphorylated S33 and S37 sites is called "active β-catenin." (Gottardi & Gumbiner, 2004) (Grigoryan et al., 2008)

The cellular prion protein (PrP^c) is a key protein of many neurological diseases usually secreted as a glycosylphosphatidyl inositol-anchored glycoprotein associated with lipid raft microdomains of the plasma membrane. (Vey et al., 1996). Although there has been a relatively large amount of research on diseases caused by PrP^c isoform and related to stem cell, the biological role of PrP^c has not yet been elucidated. Normally, PrP^c is expressed in various cell types, where it is also contributed to regulating cell proliferation, differentiation,

survival, adhesion, and signaling. (Mouillet-Richard et al., 2000)

Previously, it is suggested that there is the cooperation between Wnt and PrP^c in some tissue such as intestinal tissue and colorectal cancer (CRC). Besides, PrP^c can increase the transcriptional activity of the β-catenin/tcf7l2 complex in intestinal epithelial cells and act as a modulator of Wnt signaling. (Besnier et al., 2015) Wnt-β-catenin signaling is a regulator of prnp expression in colorectal cancer (CRC), and these two act by forming a positive feedback loop. (Mouillet-Richard et al., 2024). Although the interaction between the canonical Wnt pathway and PrP^c has been revealed in various tissues, it has not yet been revealed in the pregnant uterus.

Decidualization, the remolding process of the endometrium that occurs during early pregnancy, is a crucial process for embryo implantation and placenta formation in mice. In response to the implanting conceptus, endometrial fibroblast-like cells in the mouse uterus differentiate into large decidual cells. (Abrahamsohn & Zorn, 1993) This process begins with cells in the anti-mesometrial region of the endometrium, close to the implantation site. This region is called the primary decidual zone (PDZ), and it progresses toward the myometrium and mesometrial region of the uterus. This region is called the secondary decidual zone (SDZ). During decidualization, ovarian steroid hormones, called estrogen and progesterone, are tightly regulated in a time-dependent manner. This results in the regulation of the expression of genes that affect the proliferation and differentiation of uterine epithelial cells and stromal cells according to the hormonal cycle (Dey et al., 2004). Estrogen induces endometrial proliferation, and Progesterone induces morphological and functional changes in the endometrium occur and promote shift from the

proliferative phase to the secretory phase. Then, the uterus endometrium becomes ready to accept the embryo. Although the exact molecular mechanism has not yet been elucidated, it is thought that various genes play an important role during the decidualization process.

In addition to natural pregnancy decidualization (NPD), the artificial decidualization (AD) model is an essential model for studying the physiological and molecular mechanisms during decidualization. NPD and AD have only a little difference in morphology. The disappearance of the uterine glands of the endometrium after decidualization is same, and there is no significant difference in gene expression levels. Therefore, the artificial decidualization model is also appropriate for exploring unknown pathogenesis or new treatments for human reproductive diseases. (De Clercq et al., 2017; Wang et al., 2020)

Human cells have genes encoding approximately 20,000 proteins. Their transcriptomes are much more complex, with approximately 82,141 distinct mRNA sequences entered in the latest version of GENCODE. (Frankish et al., 2015., Harro2 et al., 2012., Biamonti et al., 2014) In high eukaryotes especially in human and mouse, many genes can produce multiple isoforms of protein products through alternative splicing (AS) of their mRNAs. Alternative splicing is a process in which a single RNA precursor produces structurally and functionally different mRNA and protein variants. This process will add proteome diversity and cellular complexity. (Climente-González et al., 2017). In addition, Alternative splicing affects the biological characteristics of proteins by adding or deleting functional domains, and modifying its stability, controlling its localization, and modifying its protein-protein interactions. (Lee & Abdel-Wahab, 2016). More importantly, genome-wide studies suggest that 92-95% of

human multi-exon genes undergo Alternative splicing. (Feng et al., 2013)

Eventhough, the alternative spliced form of β-catenin is suggested that specifically acts during the pregnant uterus decidualization process and to find out how the form affects decidualization and embryo development between prion and β-catenin using a $Prnp^{ZH3/ZH3}$ knockout mouse model.

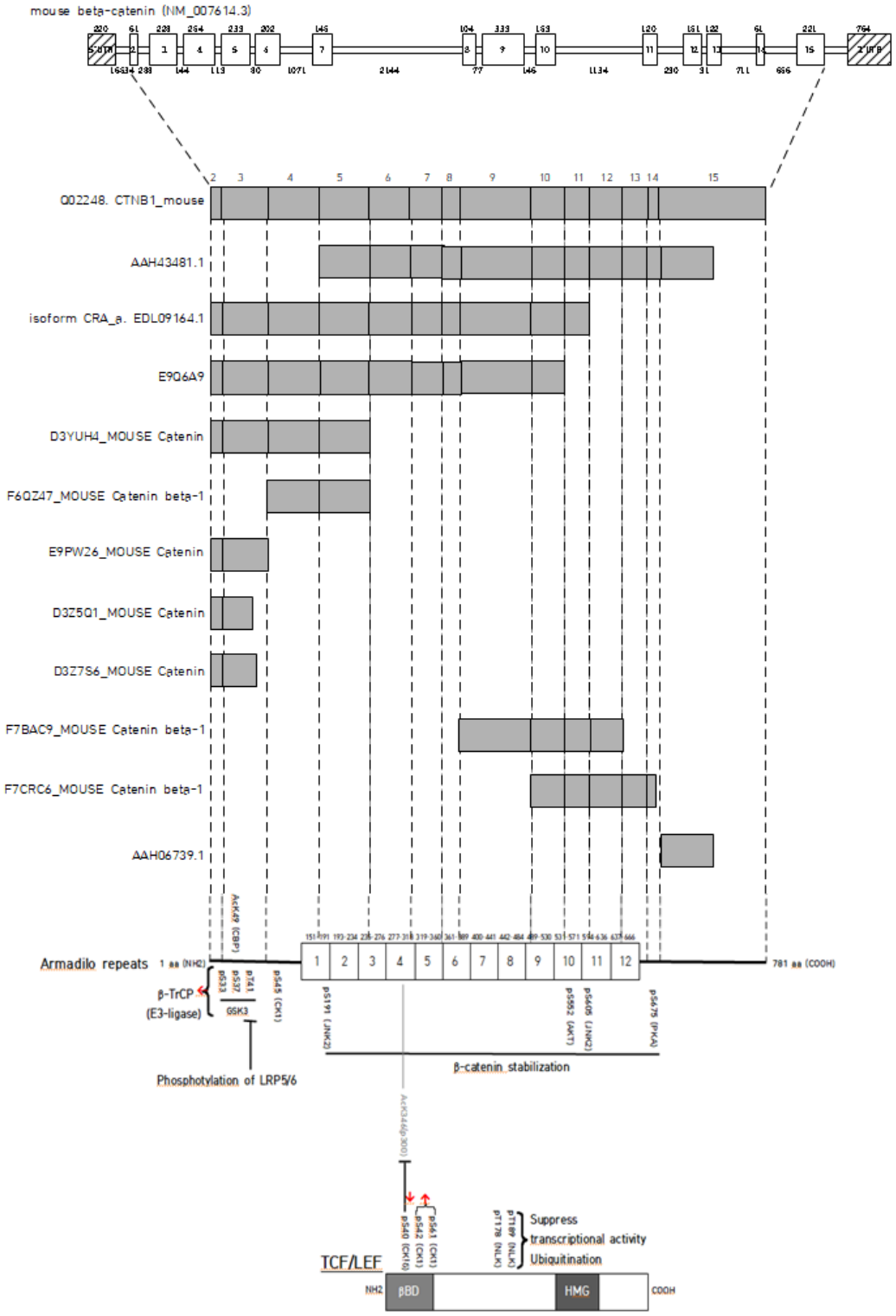
mouse beta-catenin (NM_007614.3)
Q02248. CTNB1_mouse
AAH43481.1
isoform CRA_a. EDL09164.1
E9Q6A9
D3YUH4_MOUSE Catenin
F6QZ47_MOUSE Catenin beta-1
E9PW26_MOUSE Catenin
D3Z5Q1_MOUSE Catenin
D3Z7S6_MOUSE Catenin
F7BAC9_MOUSE Catenin beta-1
F7CRC6_MOUSE Catenin beta-1
AAH06739.1
Armadilo repeats
1 aa (NH2)
781 aa (COOH)
β-TrCP
(E3-ligase)
GSK3
Phosphotylation of LRP5/6
β-catenin stabilization
TCF/LEF
Suppress
transcriptional activity
Ubiquitination
NH2
βBD
HMG
COOH

Figure 1. Gene Anatomy of β-catenin (CTNNB1) gene and major functional domain of its protein.

Uniprot information based putative β-catenin isoforms were illustrated. If it suspected that those information are not solely show the full sequences of each one.

MATERIALS AND METHODS

Experimental animals

All animal experiments were performed in accordance with the Guide for the Care and Use of Laboratory Animals published by the National Institute of Health (NIH). Approval was granted by the Institutional Animal Care and Use Committee (IACUC) at Sungshin Women's University (SSWIACUC-2024-006). Female C57BL/6 homozygous ZH3d/d mice, aged 6–8 weeks, were maintained under a controlled light cycle (lights on at 6:00 AM, lights off at 7:00 PM) in a clean room environment. Mice were provided with a standard rodent diet and water ad libitum, beginning at 28 days of age. To collect uterine tissue at specific pregnancy stages, females were mated with fertile wild-type males and designated as Pregnant Day 1 (PD1) upon observation of a vaginal plug in the morning.

Total RNA extraction

Uterine tissues were homogenized in TRIzol® reagent (Invitrogen, Cat #15596-026, Massachusetts, USA) at a ratio of 1 mL of reagent per 0.1 g of

tissue, and samples were left at room temperature (RT) for 10 minutes. Chloroform (0.2 mL per 1 mL of TRIzol) was added, shaken vigorously for 15 seconds, and incubated at RT for 15 minutes. The mixture was centrifuged at 12,000 g for 15 minutes at 4°C, and the upper aqueous phase was transferred to a new tube. To precipitate RNA, 0.5 mL of isopropanol was added per 1 mL of TRIzol, mixed gently, and incubated at RT for 10 minutes. Samples were centrifuged at 12,000 g for 8 minutes at 4°C. The RNA pellet was washed in 1 mL of 75% ethanol, followed by centrifugation at 7,500 g for 5 minutes at 4°C. After removing the ethanol, the pellet was briefly air-dried for 20 seconds and dissolved.

cDNA synthesis

The reaction mixture consisted of 34 μl total RNA, 10 μl of MMLV 5X buffer, 1 μl of oligo(dT) primer (0.5 μg/μl), 1 μl of random primer (0.1 μg/μl), and 2 μl of dNTP mix (100 mM). The mixture was first incubated at 65℃ for 5 minutes, allowed to cool to room temperature for 5 minutes, and supplemented with 4.5 μl of DTT (100 mM), 2 μl of M-MLV Reverse Transcriptase (Promega, Cat#: M170B, Wisconsin, USA), and 1 μl of an RNase inhibitor (40 U/ml). The completed reaction was incubated at 42℃ for 1 hour, followed by heating at 70℃ for 15 minutes to terminate cDNA synthesis. The cDNA was then stored at

-20℃ until further use.

RT-PCR and Sequencing

Reverse Transcription PCR (RT-PCR) was performed using specific primers listed in Table 2 and cycling conditions outlined in Table 1. The PCR products were cloned using the Original TA-cloning kit (Bioneer, South Korea) and sequenced by Cosmogentech. The resulting sequences were matched with database entries using the BLAST GenBank search to confirm identity.

Real-time PCR analysis

To measure gene expression levels, target transcripts were amplified using reverse transcription (RT)-PCR with the specific primers listed in Table 2. Quantitative real-time RT-PCR was carried out using SYBR Premix Ex Taq™ (TaKaRa, #RR420) on the AriaMx Real-Time PCR System (Agilent, #G8830A, US). The thermal cycling parameters are provided in Table 1.

Each reaction was performed in triplicate, utilizing 1 μl of cDNA per reaction. To confirm the specificity of amplification, dissociation curves were analyzed to verify the presence of a single product with the expected melting temperature. Gene expression changes were calculated using the ΔΔCt method, with ribosomal protein 36B4 used as the internal control for normalization.

Protein extraction and Western blotting analysis

Uterine tissues were homogenized in cold homogenization buffer containing 50 mM Tris-Cl, 150 mM NaCl, 10 mM β-mercaptoethanol, 2 mM $CaCl_2$, 0.1 mM PMSF, 1 μM Leupeptin, 1 μM Pepstatin, 0.5 mM EDTA, 15% Glycerol, and 0.1% NP-40. The homogenate was centrifuged to remove insoluble debris. Protein concentrations were measured using the BCA assay kit (Thermo Fisher Scientific, #23225, US).

Protein samples (20 μg/ml) were mixed with SDS/β-mercaptoethanol sample buffer, boiled, and resolved on a 10% SDS-PAGE gel. After electrophoresis, proteins were transferred onto polyvinylidene difluoride (PVDF) membranes (Bio-Rad, #1620177) using transfer buffer (25 mM Tris base, 192 mM Glycine, 0.1% SDS, and 20% Methanol). The membranes were blocked for 1 hour at room temperature with 10% skimmed milk in TBST buffer (10 mM Tris-HCl, 150 mM NaCl, and 0.05% Tween-20), followed by three washes with TBST.

Membranes were incubated overnight at 4℃ with primary antibodies (as detailed in Table 3). Afterward, the membranes were washed three times and incubated for 1 hour at room temperature with horseradish peroxidase (HRP)-conjugated secondary antibodies: goat anti-rabbit IgG (1:2000 dilution) or goat anti-mouse IgG (1:2000 dilution). Protein bands were visualized using ECL

detection solution (Bio-Rad, #1705060, US) and imaged using the ChemiDoc MP Imaging System (Bio-Rad, #17001402, US). Band intensities were normalized to total protein levels and analyzed using ImageJ software.

Co-immunoprecipitation

Protein samples (500 μg) were incubated overnight with 5 μg of rabbit monoclonal β-catenin antibody and 500 μl of homogenization buffer (50 mM Tris-Cl, 150 mM NaCl, 10 mM β-mercaptoethanol, 2 mM $CaCl_2$, 0.1 mM PMSF, 1 μM Leupeptin, 1 μM Pepstatin, 0.5 mM EDTA, 15% Glycerol, and 0.1% NP-40) while rotating. After incubation, 50 μl of Protein A/G–Agarose (Santa Cruz Biotechnology, SC-2003) was added, and the sample was rotated at 4°C for 2 hours.

The sample was then centrifuged at 12,000 g for 2 minutes at 4°C, and the supernatant was discarded. The pellet was resuspended in 1 ml of homogenization buffer and rotated for an additional 5 minutes. This washing step was repeated four times with fresh homogenization buffer. After the final wash, the supernatant was removed, and 20 μl of 2X SDS loading buffer was added. The samples were boiled at 95°C for 5 minutes. Protein complexes were analyzed by Western blotting using a mouse monoclonal prion antibody. The input sample was used at 10% for comparison.

Immunofluorescence

4 μm sections were mounted on glass slides and subjected to antigen retrieval in boiling 10mM sodium citrate buffer (pH 6.0) for 12 min. Tissues were incubated with 1% normal goat blocking serum in PBS for 2 hr. And Tissues were incubated with 0.2% Triton X-100 in PBS for 45 min, RT. And then samples were incubated with rabbit monoclonal β-catenin antibody (dilution 1:500) in blocking solution for 3 hr. Tissues were washed with PBS. Then tissues were incubated with anti-rabbit IgG conjugated Alexa Fluor 488 (dilution 1:250, Cell signaling, #4412) for 1 hr. After washing it with PBS, tissues were incubated with mouse monoclonal prion antibody (dilution 1:200) 3 hr. Then tissues were incubated with anti-mouse IgG conjugated Alexa Fluor 594 (dilution 1:250, Cell signaling #8890) for 1 hr. Tissues were washed and incubated with DAPI staining solution (dilution 1:1000) for 30 min. Lastly, tissues were washed and mounted with Fluoremount Aqueous mounting medium (Sigma, #F4680). Fluorescence signal was imaged on LSM700 confocal microscope (Carl Zeiss).

Artificially induced decidualization

Ovariectomized (OVX) mice underwent hormonal treatments to induce decidualization. Each mouse received subcutaneous injections of 100 ng of

estradiol-17 (E2) daily for three consecutive days (three mice per genotype). After a 2-day rest period, mice were administered three daily subcutaneous injections of 1 mg progesterone (P4) combined with 6.7 ng E2.

Six hours after the final hormone injection, mechanical trauma was induced by scratching the antimesometrial uterine lumen with a needle. Mice then received daily subcutaneous injections of 1 mg P4 and 6.7 ng E2 for an additional five days. The uterine response to decidualization stimuli was monitored to assess the induction of a decidual reaction.

Statistics

All experiments were repeated at least three times to ensure reproducibility. Statistical significance between the control and experimental groups was assessed using the Student's *t*-test. Data were expressed as the mean ± standard error of the mean (SEM). Differences with a *P*-value of less than 0.05 were considered statistically significant. All statistical analyses were performed using IBM SPSS Statistics software.

Table 1. Real-time RT-PCR Thermal cycler schedule

Step		Temperature (℃)	Time	cycles
Hold		94	30 min	1
3 steps PCR	Denaturation	95	1 min	45
	Annealing	59	30 sec	
	Extension	72	1 min	
Dissociation	Denaturation	95	15 sec	1
	Annealing	60	30 sec	
	Extension	95	15 sec	
Hold		4	Indefinitely	1

Table 2. Primer sequences for RT-PCR

Gene	Symbol	NCBI gene reference		Primer sequence (5'-3')	Amplified length (bp)
catenin beta 1	***Ctnnb1***	NC_000075.7	S	CACCGCTGCGTGGACAAT	2458
			AS	CCATTCCCACCCTACCAAGTCT	
catenin beta 1	***Ctnnb1-intron***	NC_000075.7	S	GTCCCACATGCCTAGTGAGTGTT	
			AS	CATCCCCTTGAGAACTTCCCTC	
60S acidic ribosomal protein P0	***Rplp0 (36B4)***	NM_007475	S	CGACCTGGAAGTCCAACTACTTCCT	303
			AS	GCACCTTATTGGCCAACAGCAT	

Table 3. Antibody information

Antibody	Description	Cat #	Company
Beta-catenin	Rabbit monoclonal	Ab32572	Abcam
Prion	Mouse monoclonal	MA1-750	Invitrogen

RESULTS

Co-Localization of β-catenin and PrP^c in pregnant uterus

β-catenin exhibited comparable expression levels in the luminal epithelium (LE) and glandular epithelium (GE) from Day 1 to Day 5. In contrast, PrP^c demonstrated lower overall expression levels compared to β-catenin but maintained a similar expression profile relative to its Day 1 levels (Figure 2, Table 5). On Days 6 and 7, β-catenin expression decreased progressively from the primary-decidual zone (PDZ) to the secondary-decidual zone (SDZ) and deep zone, whereas PrP^c showed an increasing expression gradient toward the deeper zones (Figures 3–4, Table 5).

During Days 1 to 4, β-catenin was consistently expressed in both the nucleus and membrane, while PrP^c exhibited a gradual increase in nuclear expression (Figure 2A–D, Table 6). Notably, on Day 5, both β-catenin and PrP^c were strongly expressed in stromal cells compared to decidualized stromal cells. On Days 6 and 7, β-catenin was predominantly expressed in stromal cells, whereas PrP^c showed high expression in both stromal and decidualized stromal cells (Table 6).

β-catenin and PrPc displayed overlapping expression patterns in the uterus, with β-catenin localized in both the nucleus and membrane, and PrPc showing

increased nuclear localization from Days 1–4. On Day 5, both proteins co-localized strongly in stromal cells, and during Days 6–7, PrP^c maintained high expression in decidualized stromal cells where β-catenin was also present. This suggests potential co-localization of the two proteins, supporting their role in stromal differentiation during early pregnancy.

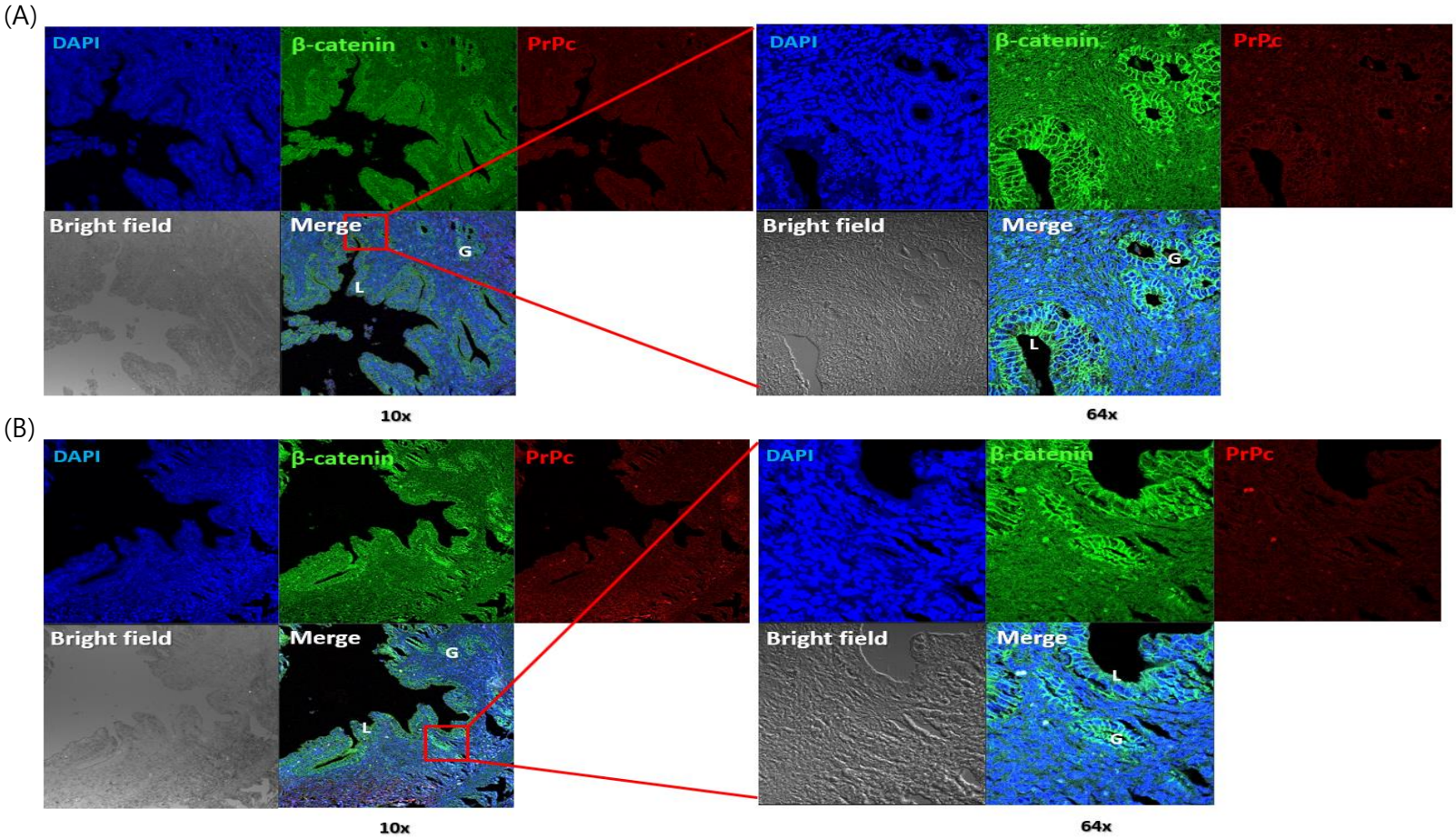
(A)
DAPI
β-catenin
PrPc
Bright field
Merge
G
L
10x
64x
(B)
DAPI
β-catenin
PrPc
Bright field
Merge
G
L
10x
64x

(C)

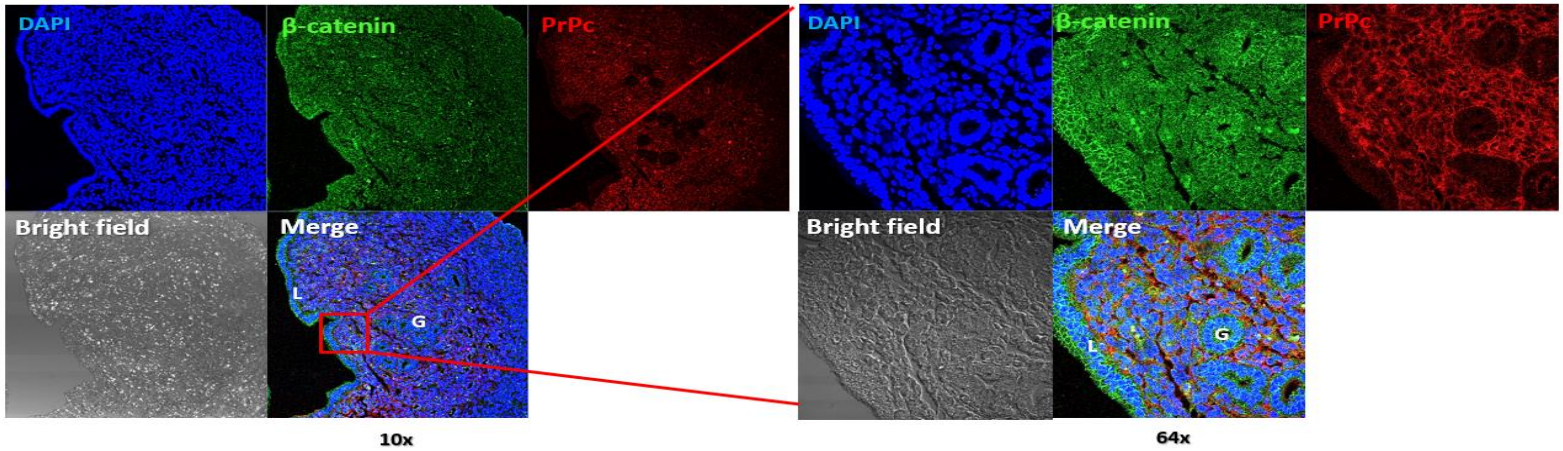
DAPI
β-catenin
PrPc
Bright field
Merge
L
G
10x
DAPI
β-catenin
PrPc
Bright field
Merge
L
G
64x

(D)

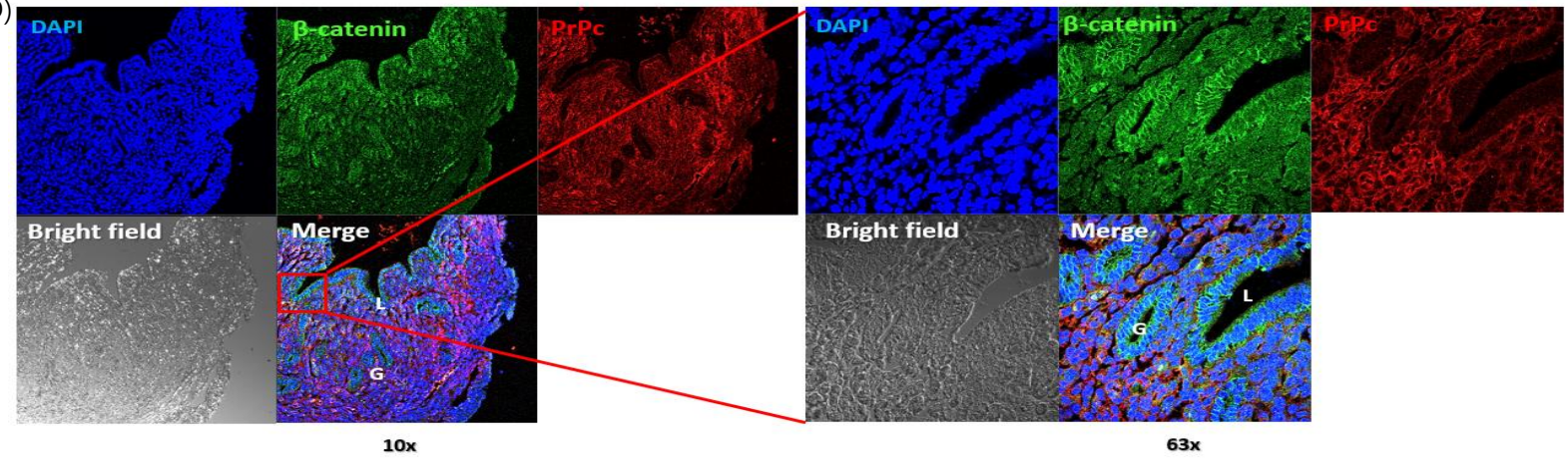
DAPI
β-catenin
PrPc
Bright field
Merge
L
G
10x
DAPI
β-catenin
PrPc
Bright field
Merge
L
G
63x

(E)

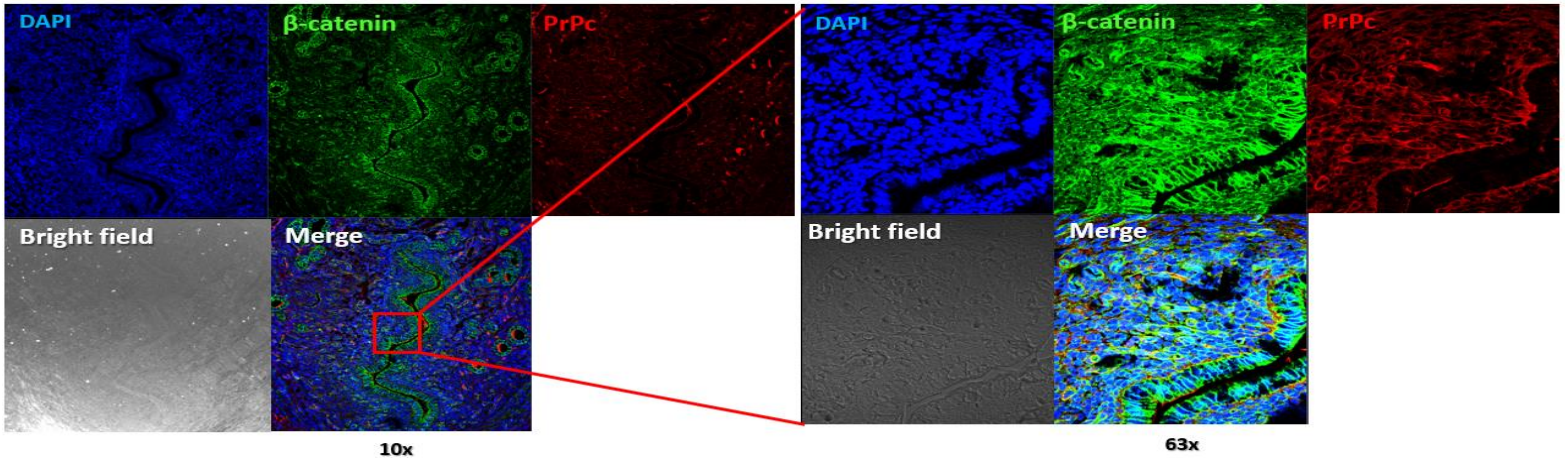

Figure 2. Localization of β-catenin and PrP^c in WT mouse PD1 - PD5 uterus

Natural pregnant uterus were performed immunofluorescence staining. Every slide costained with each β-catenin (green) and PrP^c (red), and the nuclear marker, DAPI (blue). (A) Pregnant day (PD) 1 uteri, (B) PD2, (C) PD3, (D) PD4, and (E) PD5 are wild type results. L : Luminal epithelium, G : Glandular epithelium, E : Embryo. Magnification : X100, X630.

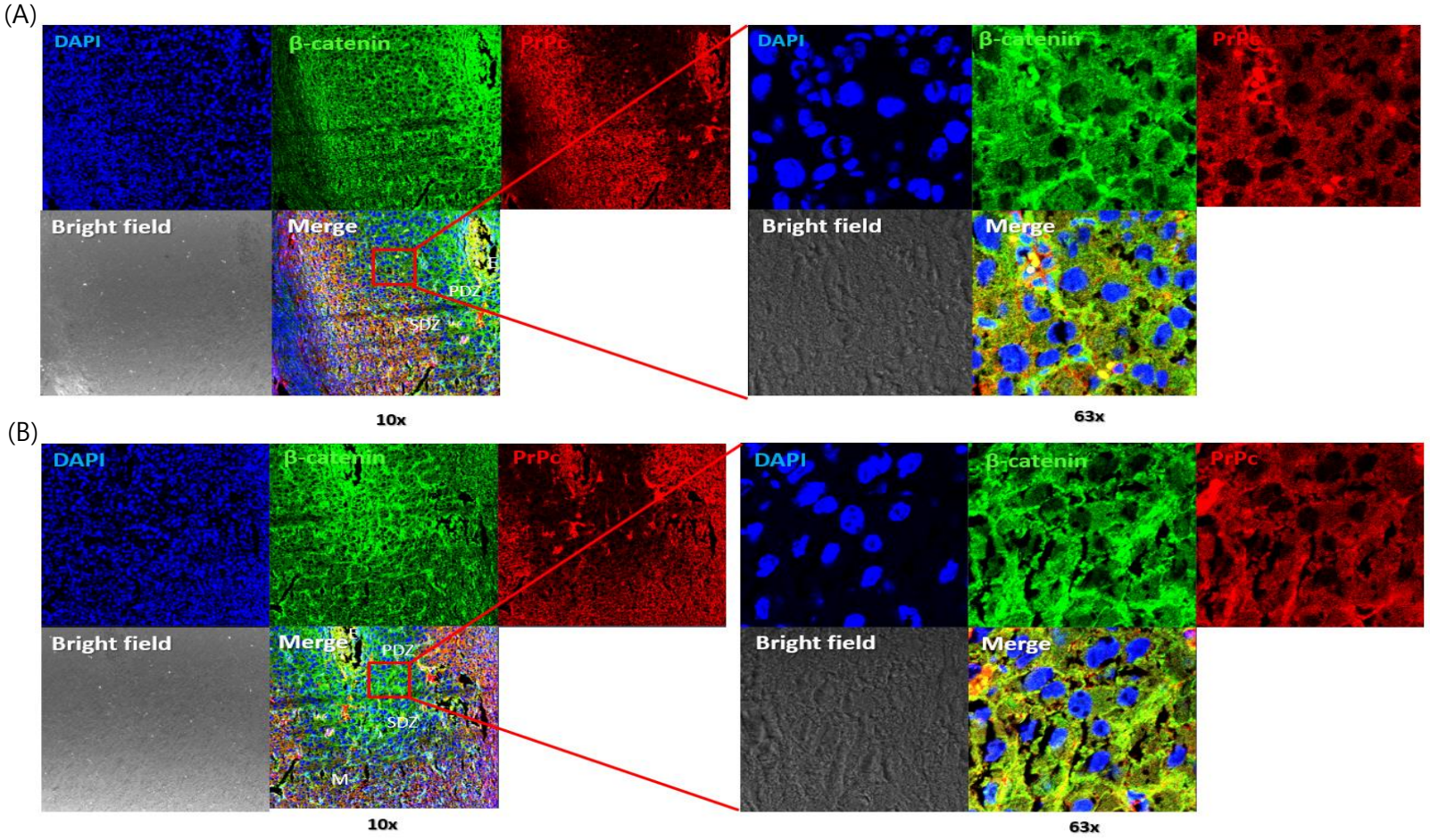
(A)
DAPI
β-catenin
PrPc
Bright field
Merge
PDZ
SDZ
10x
DAPI
β-catenin
PrPc
Bright field
Merge
63x
(B)
DAPI
β-catenin
PrPc
Bright field
Merge
PDZ
SDZ
M
10x
DAPI
β-catenin
PrPc
Bright field
Merge
63x

(C)

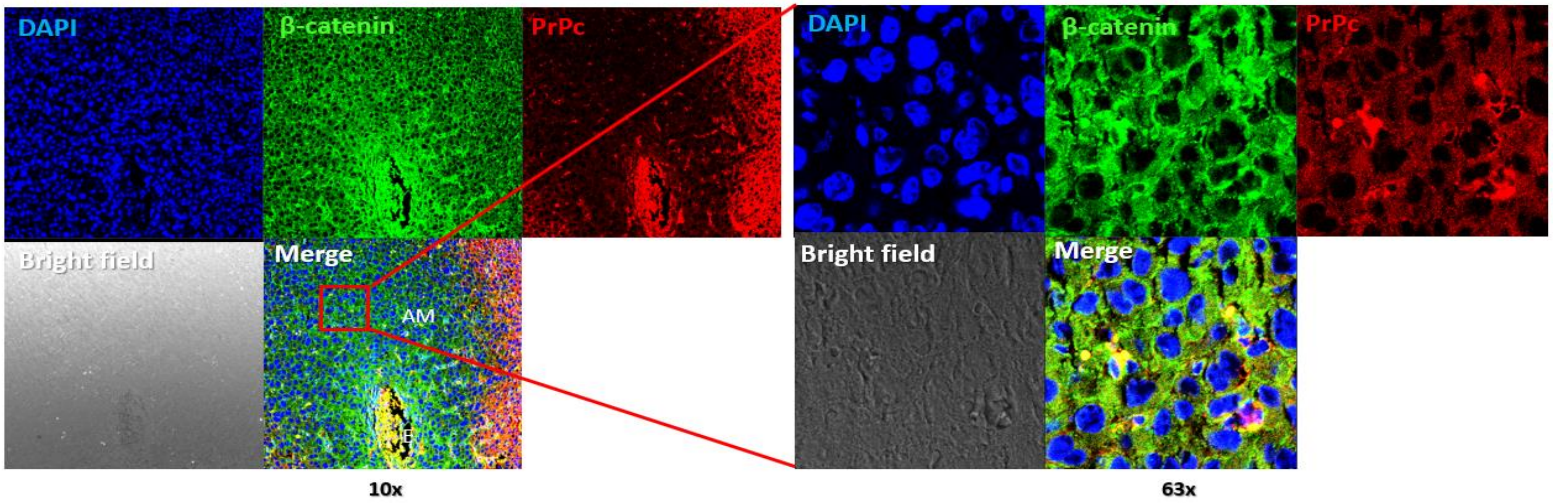

Figure 3. Localization of β-catenin and PrP^{c} in WT mouse PD6 uteri

Natural pregnant uterus were performed immunofluorescence staining. Every slide costained with each β-catenin (green) and PrP^{c} (red), and the nuclear marker, DAPI (blue). (A), (B) Mesometrial region of PD6 uteri, (C) Anti-mesometrial region of PD6 uteri are wild type results. L : Luminal epithelium, G : Glandular epithelium, E : Embryo, AM : Anti-Mesometrial region, M : Mesometrial region, PDZ : Primary Decidual Zone, SDZ : Secondary Decidual Zone. Magnification : X100, X630.

(A)

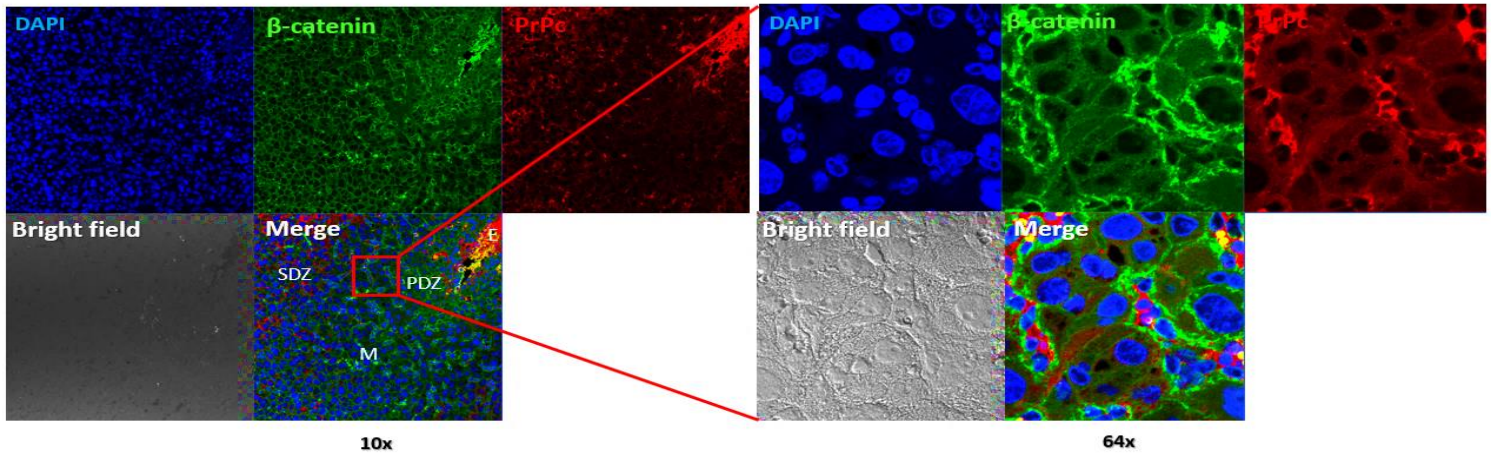
DAPI
β-catenin
PrPc
DAPI
β-catenin
PrPc
Bright field
Merge
E
SDZ
PDZ
M
Bright field
Merge
10x
64x

(B)

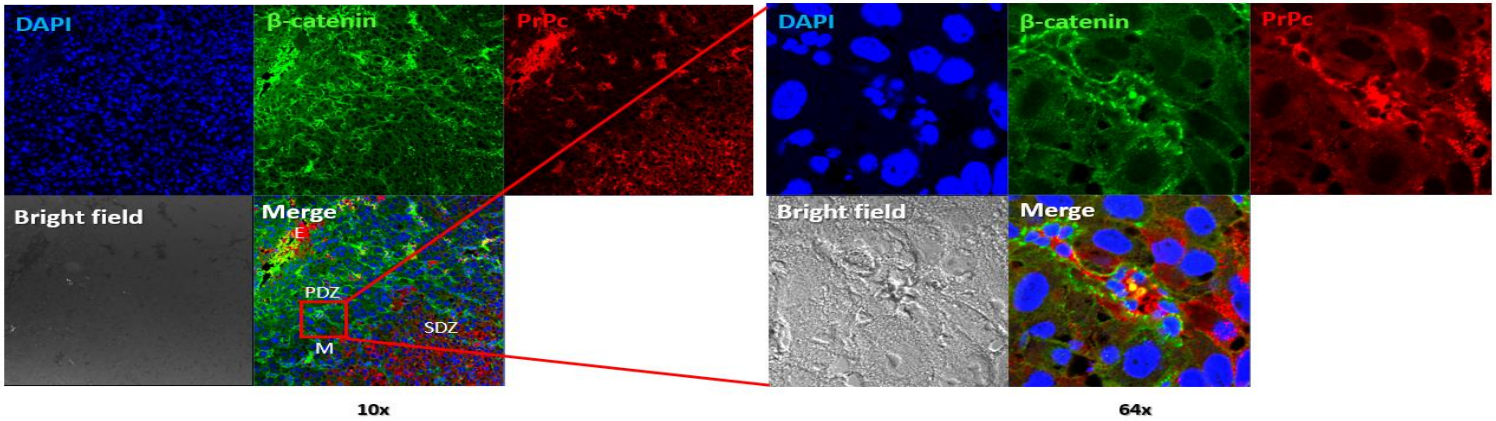
DAPI
β-catenin
PrPc
DAPI
β-catenin
PrPc
Bright field
Merge
E
PDZ
SDZ
M
Bright field
Merge
10x
64x

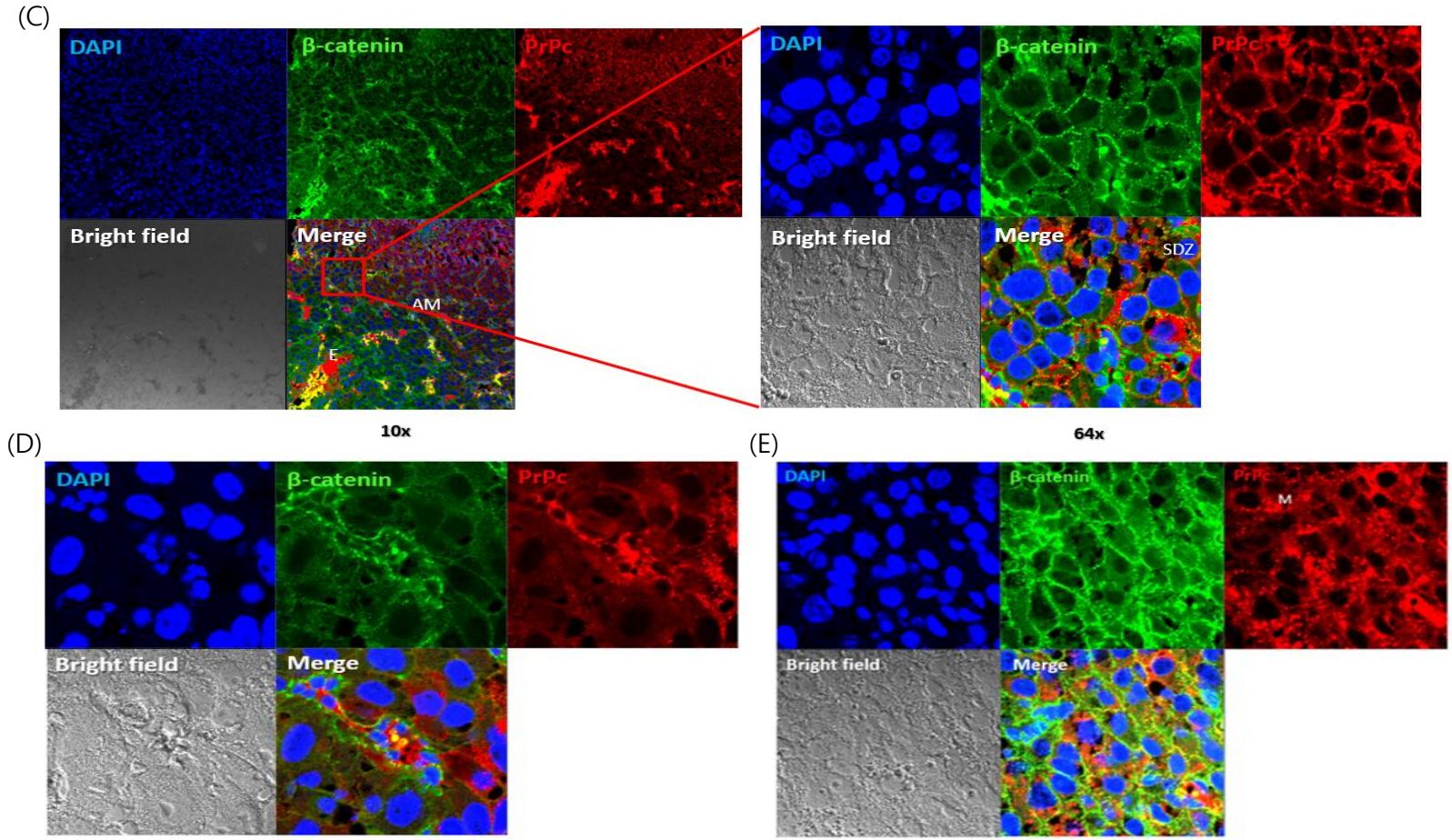
(C)
DAPI
β-catenin
PrPc
Bright field
Merge
AM
E
10x
DAPI
β-catenin
PrPc
Bright field
Merge
SDZ
64x
(D)
DAPI
β-catenin
PrPc
Bright field
Merge
(E)
DAPI
β-catenin
PrPc
M
Bright field
Merge

(F)

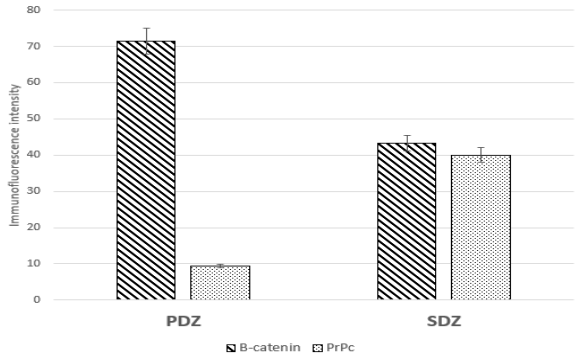

Figure 4. Localization of β-catenin and PrP^c in WT mouse PD7 uteri

Natural pregnant uterus were performed immunofluorescence staining. Every slide costained with each β-catenin (green) and PrP^c (red), and the nuclear marker, DAPI (blue). (A), (B) Mesometrial region of PD7 uteri, (C) Anti-mesometrial region of PD7 uteri are wild type results. (D) Primary decidual zone of mesometrial region of PD7 uteri, (E) Secondary decidual zone of mesometrial region of PD7 uteri, (F) Normalization of PDZ, SDZ immunoflurorescent level. L : Luminal epithelium, G : Glandular epithelium, E : Embryo, AM : Anti-Mesometrial region, M : Mesometrial region, PDZ : Primary Decidual Zone, SDZ : Secondary Decidual Zone. Magnification : X100, X630.

(A)

	Luminal Epithelium		Glandular Epithelium	
	β-catenin	PrPc	β-catenin	PrPc
Day1	++	++	++	++
Day2	+++	+++	+++	+++
Day3	++	++	+	++
Day4	+++	+++	+++	+++
Day5	+++	+	+++	++

(B)

	PDZ		SDZ		Deep zone	
	β-catenin	PrPc	β-catenin	PrPc	β-catenin	PrPc
Day6	++	++	+	+++	+	+++
Day7	++	++	+	+++	+	+++

Table 4. Normalization of LE, GE, PDZ, and SDZ immunoflurorescent level

Normalization of LE, GE, PDZ, and SDZ immunoflurorescent level. (A) The fluorescence intensity was categorized based on comparison with Day 1 values: intensities greater than 1 were marked as "+++," values between 0.8 and 1 as "++," and those less than 0.8 as "+." (B) The fluorescence intensity of PDZ was categorized by comparison with the values for each Day: intensities greater than 1 were labeled as "+++," values between 0.8 and 1 as "++," and those less than 0.8 as "+." LE : Luminal Epithelium, GE : Glandular Epithelium, PDZ : Primary Decidual Zone, SDZ : Secondary Decidual Zone.

B-catenin	nucleus	membrane		PrPc	nucleus	membrane
Day1	++	++		Day1	++	++
Day2	+++	++		Day2	+++	+++
Day3	+++	+		Day3	+++	+
Day4	+	+		Day4	++++	++
Day5	++++	+++	Stromal cell	Day5	++++	+
Day6	++++	+		Day6	++++	+
Day7	++++	++		Day7	++++	++++
Day5	+++		Decidualized cell	Day5	+	
Day6	+++			Day6	+++	
Day7	+++			Day7	++++	

Table 5. Normalization of nucleus, membrane immunoflurorescent level in stromal cell and decidualized cell

Normalization of nucleus, membrane immunoflurorescent level in stromal cell and decidualized cell. The fluorescence intensity was categorized based on comparison with the Day 1 values: intensities greater than 2 were labeled as "++++," those greater than 1 but less than or equal to 2 as "+++," values between 0.8 and 1 as "++," and those less than 0.8 as "+."

β-catenin and PrP^c form a complex to facilitate mouse uterus implantation

To investigate whether β-catenin and PrP^c form a functional complex during implantation, co-localization of these proteins in the uterus was first observed. To assess this, co-immunoprecipitation experiments were performed using protein extracts from the Wild-Type (WT) pregnant Day 7 (PD7) uterus. Immunoprecipitation with an anti- β-catenin antibody was followed by western blot analysis with an anti-PrP^c antibody. This analysis confirmed the presence of PrP^c in the protein fraction immunoprecipitated with the anti- β-catenin antibody, indicating the formation of a β-catenin–PrP^c complex. These findings strongly suggest that the β-catenin–PrP^c complex plays a critical role in implantation during WT PD7 uterine development. (Figure 5)

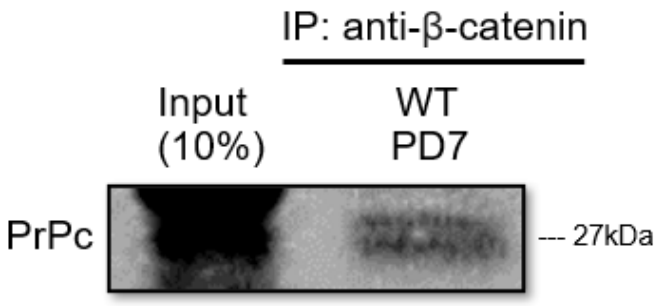

Figure 5. Co-immunoprecipitation of β-catenin and PrP^c in WT mouse PD7 uterus

Pregnant day 7 wild type mouse uterus performed co-immunoprecipitation with β-catenin with PrP^c antibody.

Essential role of PrP^c in decidualization and associated changes in β-catenin expression

To investigate the role of PrP^c and β-catenin in decidualization, we utilized $Prnp^{ZH3/ZH3}$ KO mice, in which exon 3 of the *Prnp* gene (encoding PrP^c) was completely knocked out. Co-localization and complex formation of β-catenin and PrP^c had been previously confirmed in the pregnant uterus, prompting further analysis of their functional significance during decidualization.

WT and $Prnp^{ZH3/ZH3}$ KO mice were ovariectomized and treated with E2 for three consecutive days, followed by a two-day resting period. Subsequently, a combination of E2 and P4 was administered for seven days, with mechanical trauma applied to the uterus at 15:00 on Day 3. Six hours after the final injection, the uteri were collected for analysis. WT mice exhibited robust artificial decidualization, whereas $Prnp^{ZH3/ZH3}$ KO mice showed significantly reduced decidual responses. (Figure 6)

Decidualization markers (*Igfbp1, CebpB, Prl8a2,* and *Gja1*) were analyzed using qPCR, confirming reduced expression in $Prnp^{ZH3/ZH3}$ KO mice. (Figure 7) Western blot analysis further revealed that β-catenin expression was downregulated in $Prnp^{ZH3/ZH3}$ KO mice. (Figure 8)

Immunofluorescence (IF) analysis supported these findings, showing distinct differences in the morphology and fluorescent intensity of β-catenin between WT and $Prnp^{ZH3/ZH3}$ KO mice. In the WT artificially decidualized (AD) uterus, large, rounded, multinucleated decidualized cells were prominently observed, whereas the $Prnp^{ZH3/ZH3}$ KO AD uterus exhibited smaller cells with reduced abundance (Figures 9 and 10). Additionally, the fluorescence intensity in both the luminal and glandular epithelium was lower in the $Prnp^{ZH3/ZH3}$ KO AD and KO non-decidualized uteri compared to the WT non-decidualized uterus (Figures 9 and

10, Table 5). These findings suggest that the loss of PrP^C impairs decidualization, as evidenced by the altered cellular morphology and decreased fluorescence intensity.

(A)

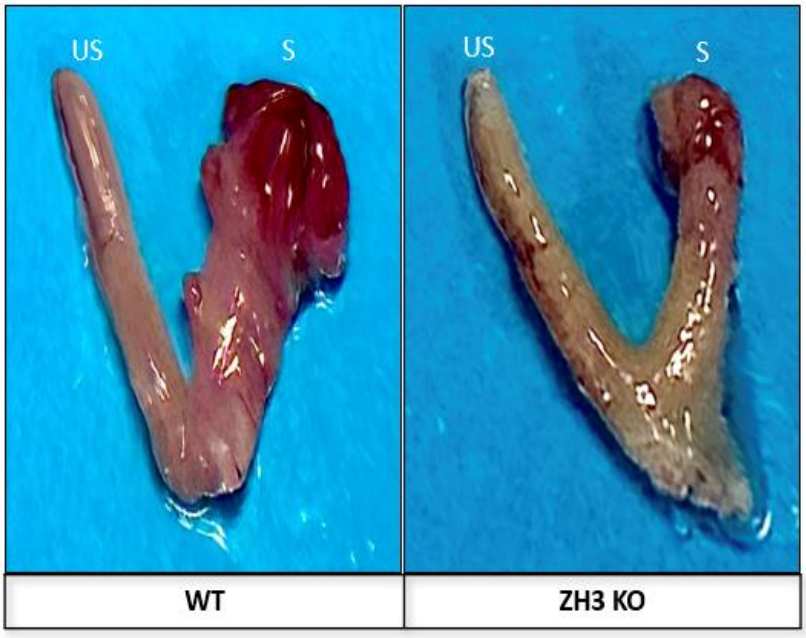
US
S
US
S
WT
ZH3 KO

(B)

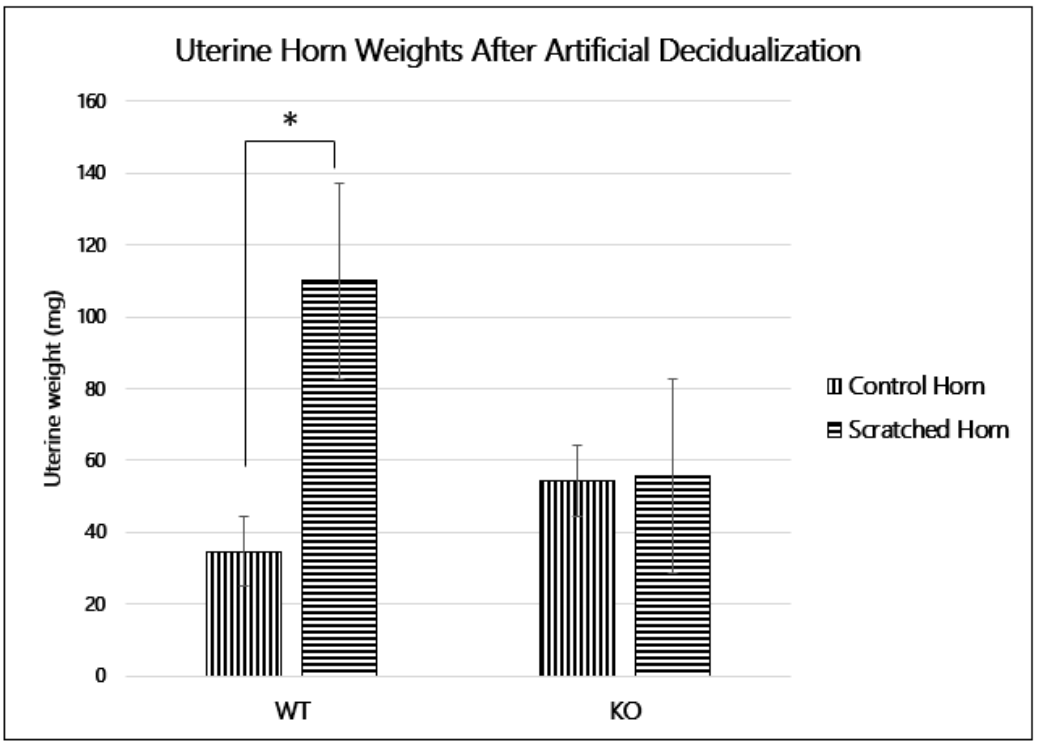
Uterine Horn Weights After Artificial Decidualization
Uterine weight (mg)
160
140
120
100
80
60
40
20
0
*
WT
KO
Control Horn
Scratched Horn

Figure 6. Images and Uterine Weight of WT and $Prnp^{ZH3/ZH3}$ KO Mice Following Artificially Induced Decidualization

Artificially Induced Decidualization in WT and $Prnp^{ZH3/ZH3}$ KO Mice uterus. (A) Representative images of uteri from WT and $Prnp^{ZH3/ZH3}$ KO mice with artificially induced decidualization. (B) Uterine weights of the control horn and scratched horn were measured in both WT and $Prnp^{ZH3/ZH3}$ KO mice. US : Un-Stimulated uterine horn, S : Stimulated uterine horn, * : $p < 0.05$ (control horn vs scratched horn).

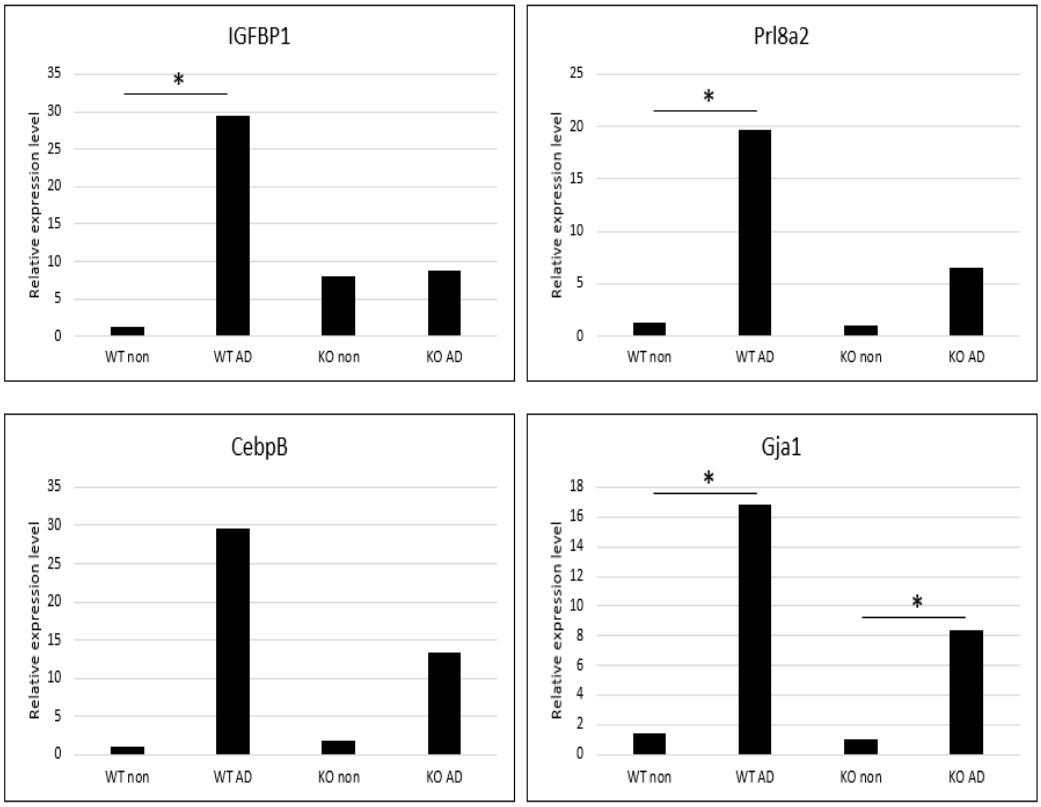

Figure 7. qRT-PCR anaylsis with decidualized marker of WT and Prnp$^{ZH3/ZH3}$ KO Mice Following Artificially Induced Decidualization

Artificially Induced Decidualization in WT and Prnp$^{ZH3/ZH3}$ KO Mice uterus was analyzed by qRT-PCR with decidualized marker. AD; Artificial decidualized uterine horn, non; non-decidualized uterine horn * : $p < 0.05$.

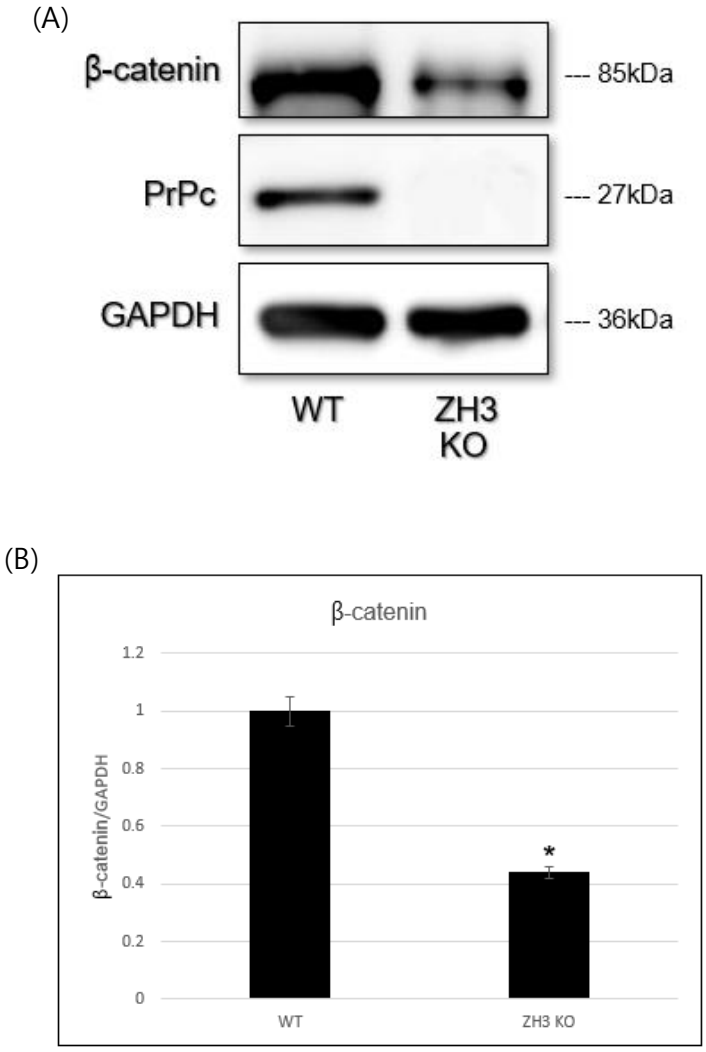

Figure 8. Western blotting of WT and Prnp$^{ZH3/ZH3}$ KO Mice Following Artificially Induced Decidualization

Artificially Induced Decidualization in WT and Prnp$^{ZH3/ZH3}$ KO Mice uterus. (A) Western blotting of uteri from WT and Prnp$^{ZH3/ZH3}$ KO mice with artificially induced decidualization. (B) B-catenin intensity were normalized in both WT and Prnp$^{ZH3/ZH3}$ KO mice by GAPDH. * : $p < 0.05$ (WT vs ZH3 KO)

(A)

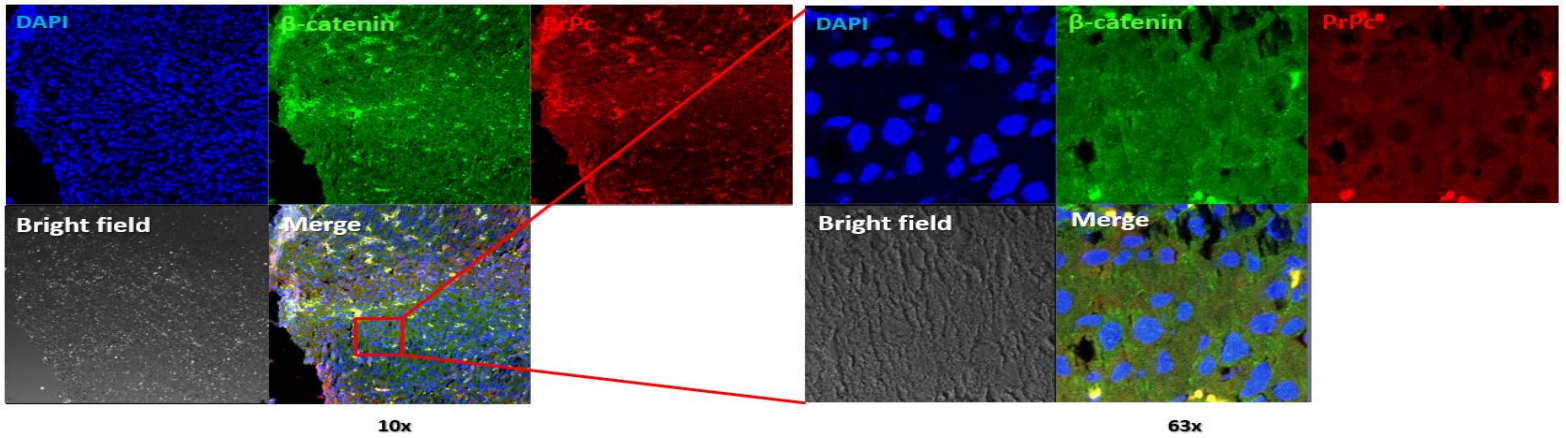
DAPI
β-catenin
PrPc
Bright field
Merge
DAPI
β-catenin
PrPc
Bright field
Merge
10x
63x

(B)

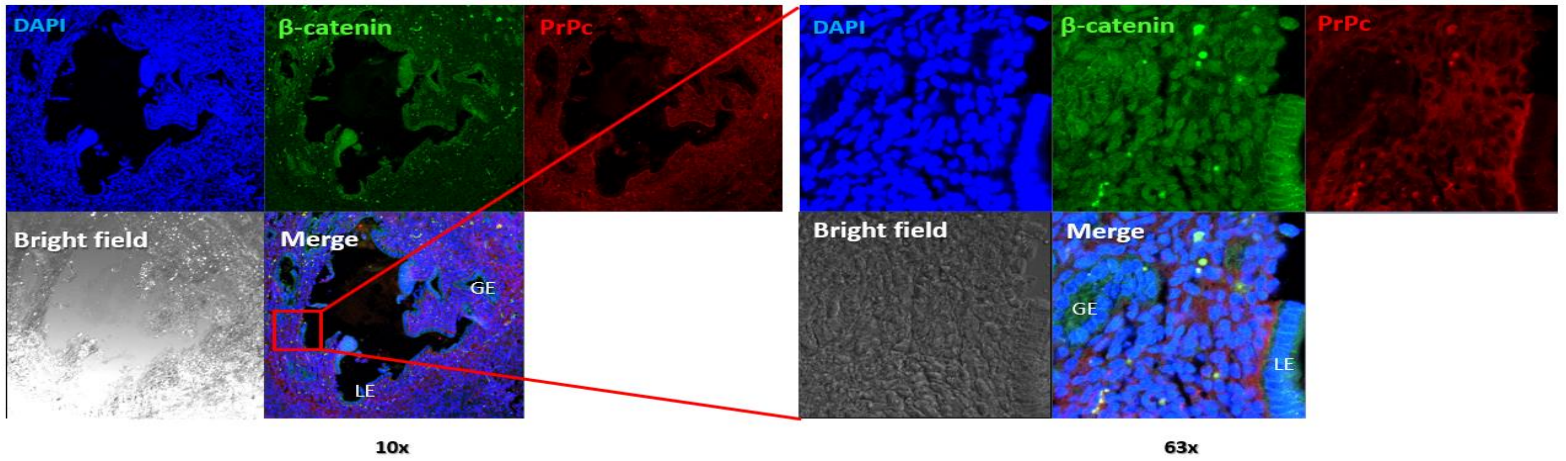
DAPI
β-catenin
PrPc
Bright field
Merge
GE
LE
DAPI
β-catenin
PrPc
Bright field
Merge
GE
LE
10x
63x

Figure 9. Localization of β-catenin and PrP^c in WT artificial decidualized mouse uterus

WT mouse uterus were performed immunofluorescence staining. Every slide costained with each β-catenin (green) and PrP^c (red), and the nuclear marker, DAPI (blue). (A) Artificially decidualized mouse uterus, (B) non-decidualized mouse uterus are wild type results. LE : Luminal epithelium, GE : Glandular epithelium. Magnification : X100, X630.

(A)

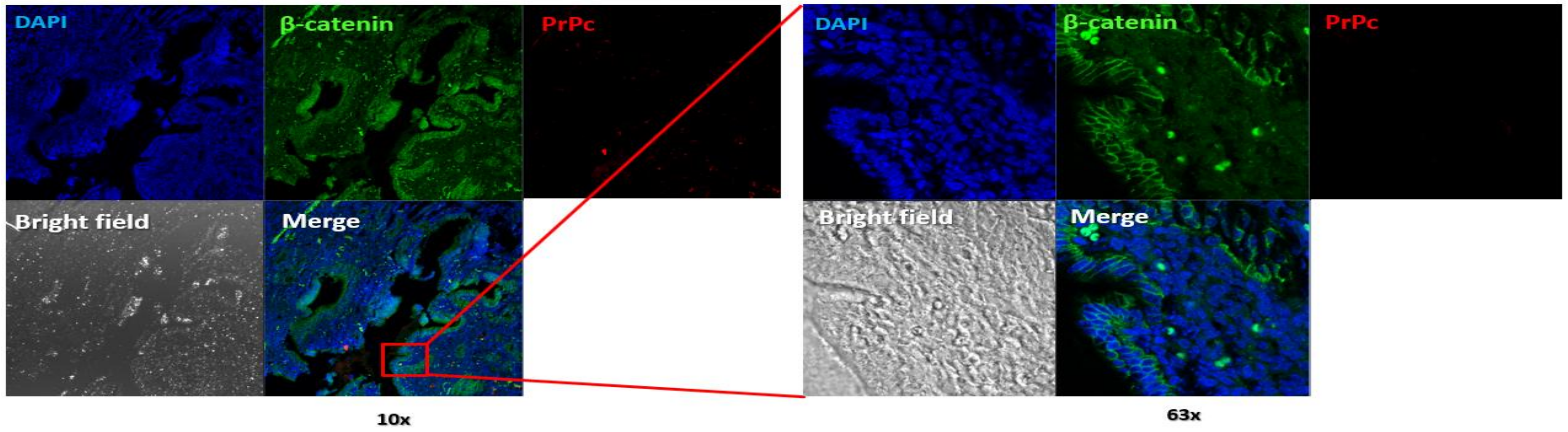
DAPI
β-catenin
PrPc
Bright field
Merge
10x
DAPI
β-catenin
PrPc
Bright field
Merge
63x

(B)

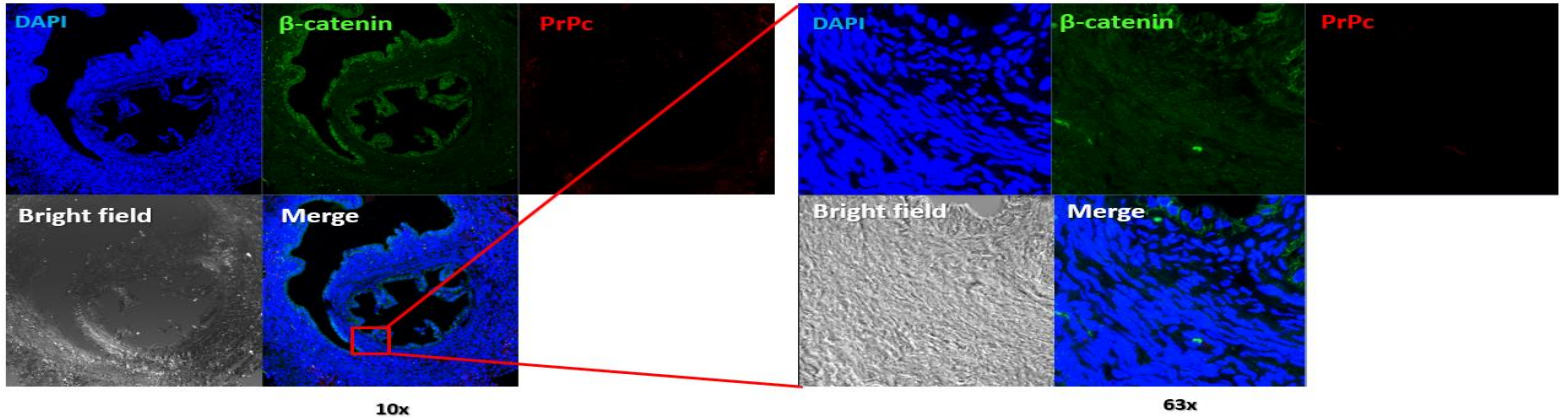
DAPI
β-catenin
PrPc
Bright field
Merge
10x
DAPI
β-catenin
PrPc
Bright field
Merge
63x

Figure 10. Localization of β-catenin and PrP^c in $Prnp^{ZH3/ZH3}$ KO artificial decidualized mouse uterus

$Prnp^{ZH3/ZH3}$ KO mouse uterus were performed immunofluorescence staining. Every slide costained with each β-catenin (green) and PrP^c (red), and the nuclear marker, DAPI (blue). (A) Artificially decidualized mouse uterus, (B) non-decidualized mouse uterus are $Prnp^{ZH3/ZH3}$ KO results. LE : Luminal epithelium, GE : Glandular epithelium. Magnification : X100, X630.

	Luminal Epithelium		Glandular Epithelium	
	β-catenin	PrPc	β-catenin	PrPc
WT AD	+++	+++	+++	+++
WT non	++	++	++	++
KO AD	+	-	+	-
KO non	++	-	+	-

Table 6. Normalization of LE, GE immunoflurorescent level

Normalization of LE and GE immunoflurorescent level. The fluorescence intensity was categorized based on comparison with each WT non values: intensities greater than 1 were marked as "+++," values between 0.8 and 1 as "++," values between 0.3 and 0.8 as "+", and those less than 0.3 as"-". LE : Luminal Epithelium, GE : Glandular Epithelium

β-catenin	nucleus	membrane		PrPc	nucleus	membrane
WT non	++	++		WT non	++	++
KO non	++	+		KO non	-	-
WT AD	+++	+++		WT AD	++	+++
KO AD	+++	++	Stromal cell	KO AD	-	-
WT AD	+++			WT AD	+	
KO AD	+		Decidualized cell	KO AD	-	

Table 7. Normalization of nucleus, membrane immunoflurorescent level in stromal cell and decidualized cell

Normalization of nucleus, membrane immunoflurorescent level in stromal cell and decidualized cell. The fluorescence intensity was categorized based on comparison with each WT non values : intensities greater than 1 were marked as "+++," values between 0.8 and 1 as "++," values between 0.3 and 0.8 as "+", and those less than 0.3 as"-".

Alternative splicing forms of β-catenin during mouse implantation

Previous experiments established the critical interaction between β-catenin and PrP^c. However, it remains unclear which alternative splicing form of β-catenin interacts with PrP^c. To address this, single-cell RNA sequencing was performed on PD4 and PD7 uteri, identifying two predominant isoforms: the canonical form (ENSMUST00000007130) and the intron retention alternatively spliced form (ENSMUST00000154687). (Figure 11)

Both isoforms were primarily expressed in epithelial and stromal cells, with the intron retention form exhibiting significantly lower expression levels compared to the canonical form. To further investigate the regulatory factors influencing their expression, RT-PCR was conducted using primers targeting overlapping regions of the two isoforms on WT PD1–7 uterine cDNA. (Figure 12A) The results demonstrated that the intron retention form showed *E2-dependent* fluctuations, whereas the canonical form displayed expression changes dependent on decidualization. (Figure 12B) These findings suggest distinct regulatory mechanisms and functional roles for the two isoforms during pregnancy.

(A)

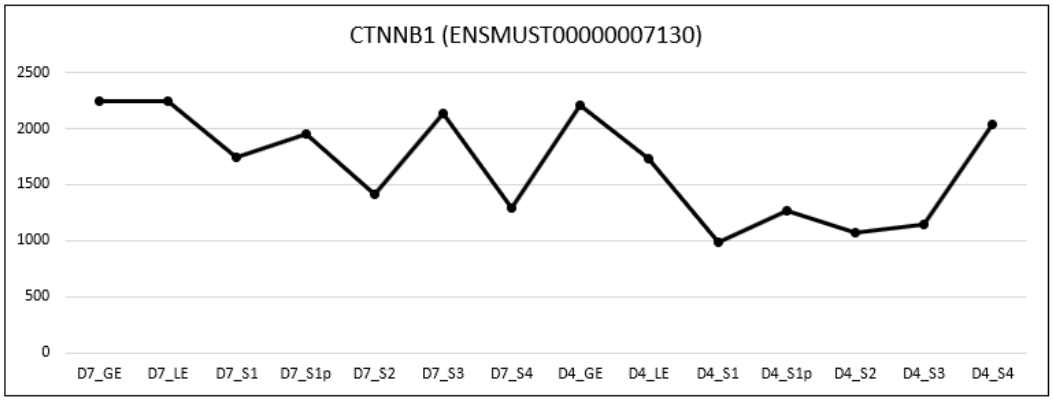

(B)

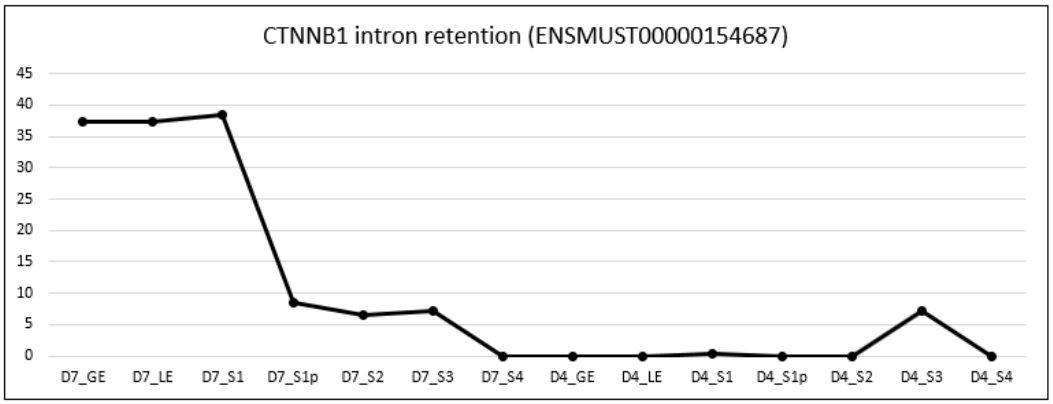

Figure 11. single cell RNA sequencing analysis about alternative splicing form of β-catenin in WT pregnant mouse uterus

single-cell RNA sequencing was performed on uteri from normal pregnant WT mice to examine the expression patterns of β-catenin on Day 4 and Day 7 of pregnancy. (A) The canonical isoform of β-catenin (ENSMUST00000007130) exhibited distinct expression patterns across different cell populations (B) An alternatively spliced isoform of β-catenin (ENSMUST00000154687), characterized by intron retention, showed a unique expression profile.

S1; superficial stromal cells, S1; proliferating superficial stromal cells, S2; deep stromal cells, S3; stromal cell3 (estimated as decidual cells), S4; stromal cell 4, LE; Luminal epithelial cells, GE; glandular epithelial cell

(A)

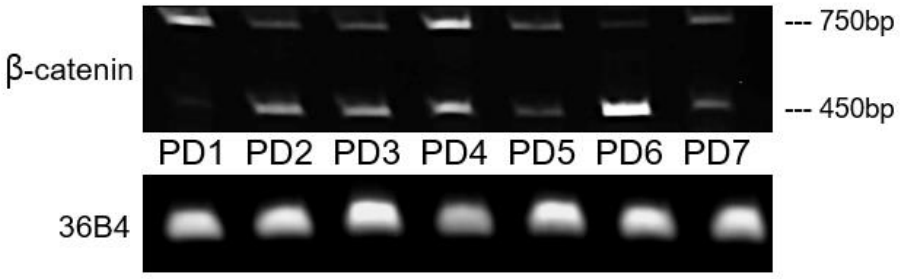

(B)

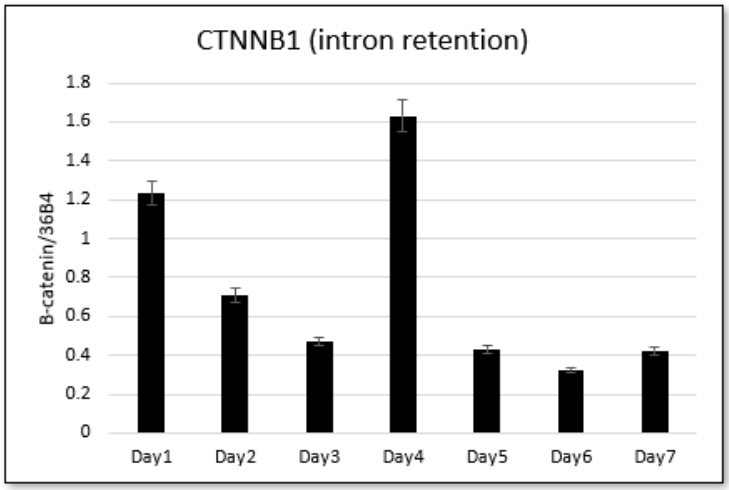

* t test vs Day3(E2-free), P<0.05

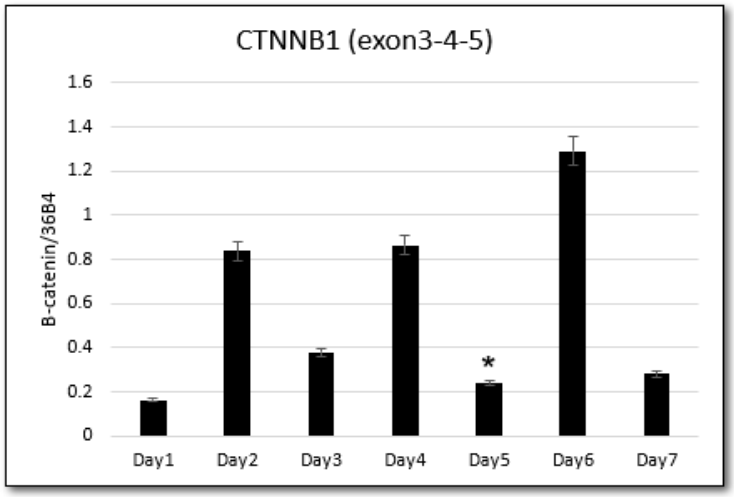

* t test vs Day1, P<0.05

Figure 12. Expression profiles of alternative splicing form of β-catenin in WT pregnant mouse uterus

To investigate the factors influencing alternative splicing forms of β-catenin, β-catenin was analyzed their expression in the uterus during pregnancy (A) PCR detection of β-catenin splicing forms was performed on uterine samples collected from Pregnant Day (PD) 1-7. (B) PCR results were normalized to housekeeping genes, allowing for quantitative comparison of splicing form expression levels during different pregnancy stages.

DISCUSSION

Implantation, a pivotal process for successful embryo implantation and placental formation, involves the differentiation of uterine stromal cells into specialized decidual cells under precise hormonal regulation. This study focuses on two key molecules, β-catenin and PrP^c, whose roles in the pregnant uterus have not been fully characterized, particularly during decidualization. β-catenin, a central mediator of the canonical Wnt signaling pathway, is well known for its roles in transcription, cell adhesion, and cellular differentiation. PrP^c, on the other hand, is a multifunctional protein traditionally associated with neurological diseases, but its emerging role in cellular signaling and proliferation has sparked interest. Although studies have revealed their interplay in other tissues, such as intestinal tissue and colorectal cancer, the relationship between β-catenin and PrP^c in the context of the pregnant uterus has remained unexplored.

Early in pregnancy, β-catenin is present in both epithelial and stromal cells, showing membrane and nuclear localization in the stromal cells during decidualization. By Day 7, its expression is strongest in the plasma membranes of decidualized stromal cells near implantation sites but diminishes as stromal cells terminally differentiate (Zhang et al., 2012). Early in pregnancy, PrP^c is present in epithelial and stromal cells. During day 6-8, PrP^c is strongly detected in PDZ, SDZ (Ding et al., 2018).

In this study, we analyzed the expression and interaction of β-catenin and PrP^c during peri-implantation. β-catenin maintained stable expression levels in the luminal epithelium (LE) and glandular epithelium (GE) from Days 1 to 5, while PrP^c exhibited lower overall expression but a similar temporal profile relative to β-catenin's Day 1 levels. This suggests that both proteins may contribute to baseline epithelial functions during early pregnancy. By Days 6 and 7, β-catenin and PrP^c displayed distinct spatial and temporal expression patterns within stromal regions. β-catenin expression progressively declined from the peri-

decidual zone (PDZ) to the sub-decidual zone (SDZ) and deep zone, suggesting its involvement in localized stromal processes near the decidualization front. In contrast, PrP^c showed an increasing gradient toward the outer uterine zones, potentially reflecting its role in broader stromal remodeling and communication between different uterine regions.

Subcellularly, β-catenin exhibited consistent nuclear and membrane localization from Days 1 to 4, aligning with its dual functions in signaling and transcription. Meanwhile, PrP^c demonstrated a gradual increase in nuclear localization, highlighting its emerging role in transcriptional regulation during mid-pregnancy. Notably, both proteins were strongly expressed in stromal cells compared to decidualized stromal cells on Day 5. However, by Days 6 and 7, β-catenin became predominantly restricted to stromal cells, while PrP^c exhibited high expression in both stromal and decidualized stromal cells. These observations suggest that PrP^c may facilitate stromal differentiation while β-catenin maintains stromal cell activity and signaling integrity.

To further explore the molecular basis of β-catenin's functions during decidualization, we investigated its alternative splicing isoforms using single-cell RNA sequencing. Two major isoforms were identified: the canonical form (ENSMUST00000007130) and the intron retention form (ENSMUST00000154687). Both were expressed predominantly in epithelial and stromal cells, but the intron retention isoform was expressed at much lower levels than the canonical form. RT-PCR analysis revealed distinct regulatory mechanisms for these isoforms: the intron retention form exhibited *E2-dependent* expression changes, while the canonical form displayed decidualization-dependent regulation. This indicates that the canonical form likely plays a dominant role in stromal differentiation and interacts with PrP^c to facilitate proper decidualization.

Using the ZH3 knockout mouse model, in which PrP^c is absent, we investigated the functional consequences of this interaction. The absence of PrP^c resulted in impaired decidualization, coupled with altered β-catenin isoform expression. Specifically, we observed downregulation of the canonical β-catenin. This

suggests that the canonical 85 kDa form of β-catenin is a key interacting partner of PrP^c during decidualization. The co-localization and complex formation of β-catenin and PrP^c were further confirmed, underscoring their functional interaction in regulating uterine stromal cell differentiation.

These findings highlight the critical interplay between β-catenin and PrP^c as transcriptional co-activators during decidualization. Their complementary spatial and temporal expression, coupled with distinct regulatory mechanisms for β-catenin isoforms, suggest a coordinated role in uterine remodeling and adaptation during early pregnancy. The artificial decidualization model provided additional insights into these molecular interactions, showing minimal differences from natural decidualization and confirming its utility for studying reproductive biology.

In conclusion, our study provides novel insights into the regulatory mechanisms underlying β-catenin and PrP^c interaction during decidualization. The distinct roles of β-catenin isoforms, particularly the canonical form, and its interaction with PrP^c underscore their importance in stromal cell differentiation and uterine remodeling. These findings lay the groundwork for future investigations into downstream pathways influenced by these proteins, as well as the broader implications for implantation, pregnancy maintenance, and potential therapeutic interventions for reproductive disorders.

REFERENCES

Abrahamsohn, P. A., & Zorn, T. M. (1993). Implantation and decidualization in rodents. *Journal of Experimental Zoology*, *266*(6), 603-628.

Besnier, L. S., Cardot, P., Da Rocha, B., Simon, A., Loew, D., Klein, C., Riveau, B., Lacasa, M., Clair, C., & Rousset, M. (2015). The cellular prion protein PrPc is a partner of the Wnt pathway in intestinal epithelial cells. *Molecular biology of the cell*, *26*(18), 3313-3328.

Biamonti, G., Catillo, M., Pignataro, D., Montecucco, A., & Ghigna, C. (2014). The alternative splicing side of cancer. Seminars in cell & developmental biology,

Climente-González, H., Porta-Pardo, E., Godzik, A., & Eyras, E. (2017). The functional impact of alternative splicing in cancer. *Cell reports*, *20*(9), 2215-2226.

De Clercq, K., Hennes, A., & Vriens, J. (2017). Isolation of mouse endometrial epithelial and stromal cells for in vitro decidualization. *Journal of visualized experiments: JoVE*(121), 55168.

Dey, S., Lim, H., Das, S. K., Reese, J., Paria, B., Daikoku, T., & Wang, H. (2004). Molecular cues to implantation. *Endocrine reviews*, *25*(3), 341-373.

Ding, N.-Z., Wang, X.-M., Jiao, X.-W., Li, R., Zeng, C., Li, S.-N., Guo, H.-S., Wang, Z.-Y., Huang, Z., & He, C.-Q. (2018). Cellular prion protein is involved in decidualization of mouse uterus. *Biology of Reproduction*, *99*(2), 319-325.

Feng, H., Qin, Z., & Zhang, X. (2013). Opportunities and methods for studying

alternative splicing in cancer with RNA-Seq. *Cancer letters*, *340*(2), 179-191.

Frankish, A., Uszczynska, B., Ritchie, G. R., Gonzalez, J. M., Pervouchine, D., Petryszak, R., Mudge, J. M., Fonseca, N., Brazma, A., & Guigo, R. (2015). Comparison of GENCODE and RefSeq gene annotation and the impact of reference geneset on variant effect prediction. *BMC genomics*, *16*, 1-11.

Gottardi, C. J., & Gumbiner, B. M. (2004). Distinct molecular forms of β-catenin are targeted to adhesive or transcriptional complexes. *The Journal of cell biology*, *167*(2), 339-349.

Grigoryan, T., Wend, P., Klaus, A., & Birchmeier, W. (2008). Deciphering the function of canonical Wnt signals in development and disease: conditional loss-and gain-of-function mutations of β-catenin in mice. *Genes & development*, *22*(17), 2308-2341.

Han, J.-h., Kim, H.-m., Seo, D.-G., Lee, G., Jeung, E.-B., & Frank, H. Y. (2015). Multiple transcripts of anoctamin genes expressed in the mouse submandibular salivary gland. *Journal of Periodontal & Implant Science*, *45*(2), 69-75.

Harrow, J., Frankish, A., Gonzalez, J. M., Tapanari, E., Diekhans, M., Kokocinski, F., Aken, B. L., Barrell, D., Zadissa, A., & Searle, S. (2012). GENCODE: the reference human genome annotation for The ENCODE Project. *Genome research*, *22*(9), 1760-1774.

Herington, J. L., Bi, J., Martin, J. D., & Bany, B. M. (2007). β-Catenin (CTNNB1) in the mouse uterus during decidualization and the potential role of two

pathways in regulating its degradation. *Journal of Histochemistry & Cytochemistry*, *55*(9), 963-974.

Kitagawa, M., Hatakeyama, S., Shirane, M., Matsumoto, M., Ishida, N., Hattori, K., Nakamichi, I., Kikuchi, A., Nakayama, K.-i., & Nakayama, K. (1999). An F-box protein, FWD1, mediates ubiquitin-dependent proteolysis of β-catenin. *The EMBO journal*, *18*(9), 2401-2410.

Lee, S. C.-W., & Abdel-Wahab, O. (2016). Therapeutic targeting of splicing in cancer. *Nature medicine*, *22*(9), 976-986.

Matsuyama, S., Whiteside, S., & Li, S.-Y. (2024). Implantation and Decidualization in PCOS: Unraveling the Complexities of Pregnancy. *International Journal of Molecular Sciences*, *25*(2), 1203.

Mohamed, O. A., Jonnaert, M., Labelle-Dumais, C., Kuroda, K., Clarke, H. J., & Dufort, D. (2005). Uterine Wnt/β-catenin signaling is required for implantation. *Proceedings of the National Academy of Sciences*, *102*(24), 8579-8584.

Mouillet-Richard, S., Ermonval, M., Chebassier, C., Laplanche, J., Lehmann, S., Launay, J., & Kellermann, O. (2000). Signal transduction through prion protein. *Science*, *289*(5486), 1925-1928.

Mouillet-Richard, S., Gougelet, A., Passet, B., Brochard, C., Le Corre, D., Pitasi, C. L., Joubel, C., Sroussi, M., Gallois, C., & Lavergne, J. (2024). Wnt, glucocorticoid and cellular prion protein cooperate to drive a mesenchymal phenotype with poor prognosis in colon cancer. *Journal of Translational Medicine*, *22*(1), 337.

Nuvolone, M., Hermann, M., Sorce, S., Russo, G., Tiberi, C., Schwarz, P., Minikel, E., Sanoudou, D., Pelczar, P., & Aguzzi, A. (2016). Strictly co-isogenic C57BL/6J-Prnp−/− mice: A rigorous resource for prion science. *Journal of Experimental Medicine*, *213*(3), 313-327.

Rider, V., Isuzugawa, K., Twarog, M., Jones, S., Cameron, B., Imakawa, K., & Fang, J. (2006). Progesterone initiates Wnt-β-catenin signaling but estradiol is required for nuclear activation and synchronous proliferation of rat uterine stromal cells. *Journal of endocrinology*, *191*(3), 537-548.

Rousset, M., Leturque, A., & Thenet, S. (2016). The nucleo-junctional interplay of the cellular prion protein: A new partner in cancer-related signaling pathways? *Prion*, *10*(2), 143-152.

Svedružić, Ž. M., Ryou, C., Choi, D., Lee, S.-H., & Cheon, Y.-P. (2024). Physiology of Cellular Prion Proteins in Reproduction. *Development & Reproduction*, *28*(2), 29.

Vey, M., Pilkuhn, S., Wille, H., Nixon, R., DeArmond, S. J., Smart, E. J., Anderson, R. G., Taraboulos, A., & Prusiner, S. B. (1996). Subcellular colocalization of the cellular and scrapie prion proteins in caveolae-like membranous domains. *Proceedings of the National Academy of Sciences*, *93*(25), 14945-14949.

Wang, C., Zhao, M., Zhang, W.-Q., Huang, M.-Y., Zhu, C., He, J.-P., & Liu, J.-L. (2020). Comparative analysis of mouse decidualization models at the molecular level. *Genes*, *11*(8), 935.

Zhang, L., Patterson, A. L., Zhang, L., Teixeira, J. M., & Pru, J. K. (2012). Endometrial stromal beta-catenin is required for steroid-dependent mesenchymal-

epithelial cross talk and decidualization. *Reproductive Biology and Endocrinology*, *10*, 1-13.

Zhang, Q., & Yan, J. (2016). Update of Wnt signaling in implantation and decidualization. *Reproductive medicine and biology*, *15*, 95-105.

정선주. (2001). $₩₩beta $-catenin 에 의한 신호전달과 그 역할 ($₩₩beta $-catenin 은 세포의 감초인가₩₩ulcorner). *한국동물학회 뉴스레터*, *18*(1), 16-25.

논문개요

탈락막 형성은 배아 이식과 태반 형성에 필수적이며, 호르몬 조절 하에 자궁 기질 세포의 분화를 포함합니다. 이 연구에서 자궁 탈락막 형성 동안 Wnt 신호 전달 경로의 핵심 효과기인 β-catenin 과 다기능 단백질인 세포성 프리온 단백질 (PrP^{c}) 역할을 탐구했습니다. β-catenin 은 1 일에서 5 일까지 상피 영역에서 안정적인 발현을 유지하는 반면, PrPc 는 낮지만 평행한 발현 패턴을 보였습니다. 6 일과 7 일에는 β-catenin 발현이 더 깊은 자궁 영역으로 감소한 반면, PrPc 는 바깥쪽 영역에서 발현이 증가하여 자궁 리모델링에서 보완적인 역할을 시사했습니다. 단일 세포 RNA 시퀀싱은 두 가지 주요 β-catenin 동형체, 표준형과 인트론 유지형을 식별했습니다. 표준형은 탈락막 형성 의존적 발현을 보인 반면, 인트론 유지형은 에스트로겐 의존적이었습니다. $Prnp^{ZH3/ZH3}$ 낙아웃 마우스 모델을 사용하여 PrPc 가 정식 β-catenin 동형체와 특이적으로 상호 작용한다는 것을 확인했습니다. PrPc 가 없는 마우스는 탈락막 형성이 손상되고 β-catenin 동형체 발현이 변화하여 이 상호 작용의 중요성을 강조했습니다. 저희의 연구 결과는 탈락막 형성 중에 β-catenin 과 PrP^{c} 간의 중요한 상호 작용을 보여주며, 자궁 기질 분화에서 β-catenin 동형체의 역할이 서로 다릅니다. 이러한 결과는 자궁 리모델링의 분자적 메커니즘에 대한 새로운 통찰력을 제공하고 착상과 임신 유지에 대한 미래 연구의 토대를 마련합니다.